Inorganic Chemistry

Article

pubs.acs.org/IC

Synthesis, Crystal Structures, and Hydrogen-Storage Properties of $Eu(AlH_4)_2$ and $Sr(AlH_4)_2$ and of Their Decomposition Intermediates, $EuAlH_5$ and $SrAlH_5$

André Pommerin, Aron Wosylus, Michael Felderhoff, Ferdi Schüth, and Claudia Weidenthaler*

Max-Planck-Institut für Kohlenforschung, Kaiser-Wilhelm-Platz 1, 45470 Mülheim, Germany

Supporting Information

ABSTRACT: Complex $Eu(AlH_4)_2$ and $Sr(AlH_4)_2$ hydrides have been prepared by a mechanochemical metathesis reaction from $NaAlH_4$ and europium or strontium chlorides. The crystal structures were solved from powder X-ray diffraction data in combination with solid-state ^{27}Al NMR spectroscopy. The thermolysis pathway was analyzed in detail, allowing identification of new intermediate $EuAlH_5/SrAlH_5$ compounds. Rehydrogenation experiments indicate that the second decomposition step is reversible.

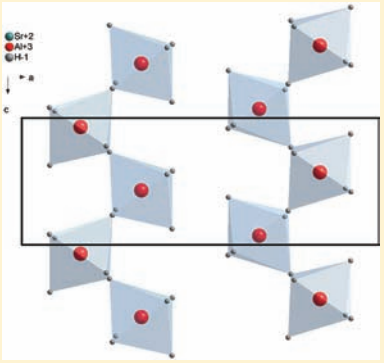

INTRODUCTION

Since the discovery by Bogdanović and Schwickardi that the complex aluminum hydride $NaAlH_4$ can be reversibly hydrogenated, complex aluminum hydrides are intensively investigated as potential solid hydrogen-storage materials.[1] Unfortunately, up to now only $NaAlH_4$ doped with different types of catalysts can be reversibly rehydrogenated under moderate physical conditions. Even though the theoretical storage capacities of other complex hydrides look encouragingly high, in most cases the dehydrogenated products cannot be rehydrogenated under reasonable conditions.[2] Therefore, the aim of our work is the preparation of new classes of complex aluminum hydrides with advantageous hydrogen-storage properties. The comprehensive characterization of the structural and thermodynamic properties is mandatory to understand the hydrogen-storage properties of complex hydrides. With knowledge about the crystal structure, thermodynamic properties, and hydrogenation processes, it should be possible to understand the mechanism of hydrogen storage in complex hydrides. On the basis of such knowledge, one day it might be feasible to adjust the properties of the storage material to the technical requirements.

Recently, we have published the preparation, crystal structures, and hydrogen desorption properties of a new class of rare-earth aluminum hydrides.[3] While these new compounds have low theoretical hydrogen contents, are expensive, and, most importantly, could not be rehydrogenated under moderate conditions, their synthesis proved that complex aluminum hydrides, beyond the known ones of the alkaline-earth and alkali elements, can be prepared by mechanochemical methods. Motivated by the successful preparation of these new compounds, an exploratory search for other rare-earth aluminum hydrides with higher atomic numbers was initiated.

To our best knowledge, so far no europium aluminum hydrides have been described, whereas the preparation and structural characterization of several strontium aluminum hydrides/deuterides have been reported.[4−6] $SrAl_2H_2$ and Sr_2AlH_7 have been obtained by hydrogenation of $SrAl_2$ and Sr_2Al at elevated temperatures and hydrogen pressures up to 7 MPa. $SrAl_2H_2$ has been synthesized from $SrAl_2$ by hydrogenation at 5 MPa H_2 pressure and temperatures below 200 °C. With increasing hydrogenation temperatures and increased hydrogen pressure, another strontium aluminum hydride of the composition Sr_2AlH_7 can be formed at 533 K and 7 MPa and a reaction time of 15 days.[5] The successful preparation was also reported by ball-milling of Sr_2Al under 0.6 MPa hydrogen pressure at 150 rpm for 2 days, followed by hydrogenation under a hydrogen pressure of 7 MPa or sintering at 533 K for an additional 2 days.[6] However, X-ray diffraction patterns show the presence of Al, SrH_2, SrO, and Fe besides Sr_2AlH_7. The preparation of the starting material $SrAl_2$ is somewhat laborious. It is obtained by arc melting of the elements.[4] As reported by Zhang et al., Sr_2AlH_7 could not be synthesized by ball-milling of SrH_2 and Al under hydrogen pressure at 7 MPa. Instead of Sr_2AlH_7, an amorphous phase was formed.[7] Further experiments, provided by the same group, demonstrated that Sr_2AlH_7 can be prepared from SrH_2 and Al at 553 K when the hydrogen pressure is above 2.93 MPa during ball-milling. The authors also report this formation reaction to be reversible with an enthalpy change of −51 kJ mol^{-1} of H_2.[8] The crystal structure

Received: November 20, 2011
Published: March 9, 2012

   dx.doi.org/10.1021/ic202492v | *Inorg. Chem.* 2012, 51, 4143−4150

of $SrAlH_5$ was predicted by first-principles calculations but has not been confirmed by experimental data so far.[9] The preparation of $Sr(AlH_4)_2$ from SrH_2 and AlH_3 by mechanochemical activation and subsequent decomposition to $SrAlH_5$ has been followed by spectroscopic methods.[10]

In this paper, we present the synthesis, characterization, and hydrogen-storage properties of europium aluminum hydride, $Eu(AlH_4)_2$, and strontium aluminum hydride, $Sr(AlH_4)_2$. The crystal structures of both alanates and of their intermediate decomposition products, $EuAlH_5$ and $SrAlH_5$, are presented as well.

EXPERIMENTAL SECTION

Because of air and moisture sensitivity of the starting materials as well as products, all operations were performed under a protecting argon atmosphere, using a glovebox or Schlenk techniques. Commercial $NaAlH_4$ (Chemetall) was recrystallized by the addition of pentane to a tetrahydrofuran (THF) solution of $NaAlH_4$. For the preparation of $Eu(AlH_4)_2$, anhydrous $EuCl_3$ and $EuCl_2$ (Aldrich 99.9%) were used without further purification. For simplification, the product prepared from $EuCl_2$ + $2NaAlH_4$ is named $Eu(AlH_4)_2$-II and the product prepared from $EuCl_3$ + $3NaAlH_4$ is named $Eu(AlH_4)_2$-III. The complex aluminum hydrides were prepared by the metathesis reaction of $EuCl_3$, $EuCl_2$, and $SrCl_2$ with sodium aluminum hydride, $NaAlH_4$. For the preparation of $Eu(AlH_4)_2$-III, 1.000 g (18.52 mmol) of $NaAlH_4$ and 1.594 g (6.17 mmol) of $EuCl_3$ were mixed. For the preparation of $Eu(AlH_4)_2$-II, 500 mg (9.26 mmol) of $NaAlH_4$ and 1.039 g (4.66 mmol) of $EuCl_2$ were reacted. $Sr(AlH_4)_2$ was synthesized by the reaction of 553 mg (9.87 mmol) of $NaAlH_4$ with 900 mg (5.68 mmol) of $SrCl_2$. For the preparation of strontium alanate, the molar ratio of $NaAlH_4$ to $SrCl_2$ was 1.8:1 with an excess of $SrCl_2$.

In a typical experiment, stoichiometric amounts of the corresponding metal chloride and $NaAlH_4$ were mixed in a glovebox. The metathesis synthesis was performed with a Fritsch Pulverisette P6 hardened stainless steel vial, using seven balls (13.9 g each) at a rotational speed of 500 rpm. Milling times were varied between several minutes up to 7 h to ensure an almost complete reaction. For this solid-state reaction, the reagents were mixed in a high-energy ball mill under increased hydrogen pressure of 0.1−1.5 MPa. For tracking of the potential decomposition processes during ball-milling, a commercial mill (Fritsch P6, 500 rpm) equipped with a telemetric system was used to observe the pressure and temperature evolution.[11] The preparation of $Sr(AlH_4)_2$ was slightly different. For complete conversion, a molar ratio of $NaAlH_4$ to $SrCl_2$ (Aldrich 99.99%) of 1.8:1, which means with a small excess of $SrCl_2$, is required. A Fritsch mill, Pulverisette P7, with a 12 mL milling vial and five balls (3.9 g each) was used. The rotational speed of 600 rpm was applied three times for 2 h and one time for 3 h of milling time. After each 2 h period, the milling vial was transferred into a glovebox, and the powder was homogenized.

Rehydrogenation was tested under different conditions: (a) with a Fritsch Pulverisette with 500 rpm at 5, 20, and 30 MPa H_2 pressure for different times and (b) under 100 MPa static H_2 pressure.

Thermal Analysis. The differential scanning calorimetry (DSC) measurements were performed on a Mettler-Toledo DSC 27HP instrument. The peak areas of the DSC curves are expressed in milliwatt units. The peak areas were calibrated on the basis of averaged heats of fusion of indium and zinc as standards. The measurements were carried out under argon, using typically 5−6 mg of the sample, and heated in an aluminum crucible with a heating rate of 10 K min^{-1}.

Thermolysis. For thermolysis, the samples were weighed into a glass vessel, and the vessel was connected to an automatic gas buret. A thermocouple allowed recording of the sample temperature during measurement. The glass vessel was inserted in an oven and heated up with 10 K min^{-1}.

X-ray Diffraction (XRD). Powder XRD experiments were performed on a Stoe STADI P transmission diffractometer using Mo Kα_1 radiation (0.709 23 Å) for the europium samples and on a STADI P transmission diffractometer using Cu Kα_1 radiation (1.540 56 Å) for the strontium samples. Both instruments are equipped with a primary monochromator and a position-sensitive detector. To protect the samples from any contact with the atmosphere, all samples were filled in a glovebox into glass capillaries (0.5 and 0.7 mm diameter), which were sealed.

Solid-State NMR Spectroscopy. The magic-angle-spinning (MAS) ^{27}Al NMR spectra were recorded on a Bruker Avance 500WB spectrometer using a double-bearing standard MAS probe (DVT BL4) at a resonance frequency of 130.3 MHz. The experimental conditions were as follows: 10 kHz spinning rate, 1200 scans, single $\pi/12$ pulses (0.6 μs), and 1 s recycle delay. The chemical shift was referenced to a 1 M aqueous solution of $Al(NO_3)_3$ in a separate rotor. The temperatures (±3 K) given for the in situ measurements refer to the hottest parts of the sample.

RESULTS AND DISCUSSION

Synthesis of $Eu(AlH_4)_2$. After different milling times, samples were investigated by powder XRD methods. After 10 min of milling, most of $NaAlH_4$ had reacted with $EuCl_3$. During this reaction, aluminum and a mixed-valent sodium europium salt of the composition $NaEu_2Cl_6$ were formed (Figure 1a).[12]

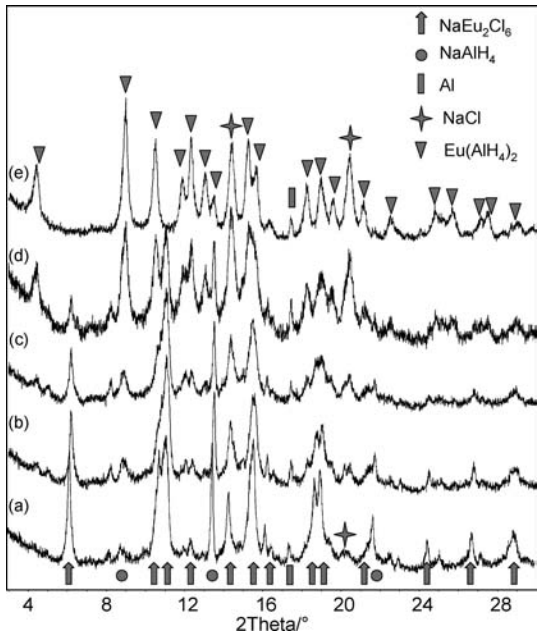

Figure 1. Milling products after ball milling of $3NaAlH_4$ and $EuCl_3$ for (a) 10, (b) 20, (c) 30, (d) 60, and (e) 180 min (Mo Kα_1 radiation).

In this compound, the oxidation states of the europium cations are II+ and III+, indicating a redox process during the ball-milling procedure. Only small amounts of NaCl are detectable. At this stage, the formation of a new hydrogen-containing phase cannot be observed. After 20 min of ball-milling, a weak reflection appears at about $2\theta = 9°$ ($d \sim 4.6$ Å), which becomes stronger with the milling time and belongs to a new rare-earth aluminum hydride structure, later shown to have the composition $Eu(AlH_4)_2$ (Figure 1). Under such milling conditions, the formation of $Eu(AlH_4)_2$ is completed after 180 min of milling time.

In order to understand the unexpected formation of $NaEu_2Cl_6$, a 1:1:1 stoichiometric mixture of NaCl, $EuCl_2$, and $EuCl_3$ was ball-milled at 600 rpm for 3 h, which resulted in the formation of the pure $NaEu_2Cl_6$ compound (see Figure S1 in the Supporting Information). This allows a rather simple explanation of the reaction pathway for the production of the

dx.doi.org/10.1021/ic202492v | Inorg. Chem. 2012, 51, 4143−4150

mixed-valent europium salt during the synthesis of $Eu(AlH_4)_2$ starting from $EuCl_3$: The first step is a simple metathesis reaction between $EuCl_3$ and $NaAlH_4$, producing sodium chloride and possibly an unstable product with the composition $[EuCl_2(AlH_4)]$ (eq 1). This compound decomposes to $EuCl_2$ and AlH_3 and releases hydrogen (eq 2), indicated by the pressure increase during the ball-milling procedure (Figure 2a).

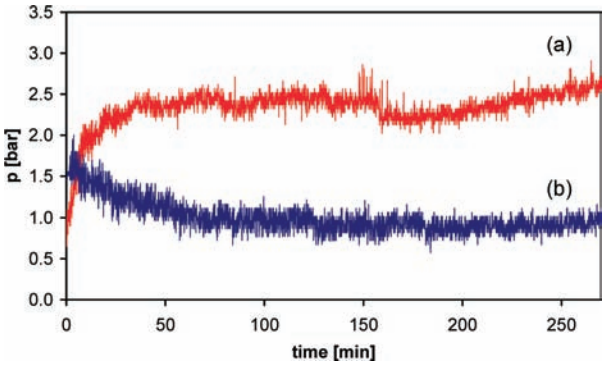

Figure 2. Hydrogen evolution curve obtained during ball-milling of (a) $3NaAlH_4 + EuCl_3$ and of (b) $2NaAlH_4 + EuCl_2$.

A pressure increase is only observed during the ball-milling of $EuCl_3$ with $NaAlH_4$ but not if $EuCl_2$ is used (Figure 2b).

$$EuCl_3 + NaAlH_4 \rightarrow [EuCl_2(AlH_4)] + NaCl \quad (1)$$

$$[EuCl_2(AlH_4)] \rightarrow EuCl_2 + AlH_3 + \frac{1}{2}H_2 \quad (2)$$

One argument for the generation of AlH_3 is the endothermic peak in the DSC measurement with an onset at about 80 °C, which is typical for the decomposition of small particles of AlH_3 (Figure 3a).[13] The $EuCl_2$ formed by the redox reaction further

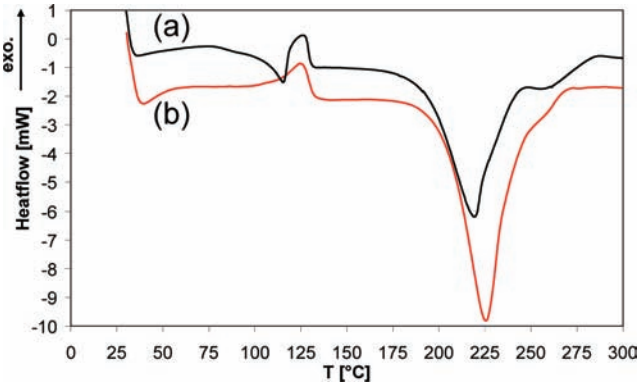

Figure 3. DSC curves for (a) $Eu(AlH_4)_2$-III and (b) $Eu(AlH_4)_2$-II. Heating rate = 10 K min^{-1}.

reacts with NaCl and $EuCl_3$, producing the mixed-valent compound $NaEu_2Cl_6$ (eq 3). Further metathesis reactions between $NaEu_2Cl_6$ and $NaAlH_4$ lead to the observed $Eu(AlH_4)_2$ material. The overall reaction sequence is summarized by eq 4.

$$EuCl_2 + EuCl_3 + NaCl \rightarrow NaEu_2Cl_6 \quad (3)$$

$$EuCl_3 + 3NaAlH_4 \rightarrow Eu(AlH_4)_2 + AlH_3 + \frac{1}{2}H_2 + 3NaCl \quad (4)$$

Previously, it was shown that significant amounts of hydrogen are released during the mechanochemical preparation of rare-earth aluminum hydrides.[3] During ball-milling of $EuCl_3$ with $NaAlH_4$, the hydrogen pressure inside the milling vessel increases, indicating the release of hydrogen. This is explained by the decomposition, and a plateau is reached already after 50 min (Figure 2a). During milling of $EuCl_2$ instead of $EuCl_3$ with $NaAlH_4$ in the stoichiometric ratio 1:2 according to the reaction (eq 5), no pressure increase is observed (Figure 2b). Analysis of the powder pattern shows that the use of $EuCl_2$ leads to the formation of $Eu(AlH_4)_2$ and NaCl without the formation of Al (Figure 4).

$$2NaAlH_4 + EuCl_2 \rightarrow Eu(AlH_4)_2 + 2NaCl \quad (5)$$

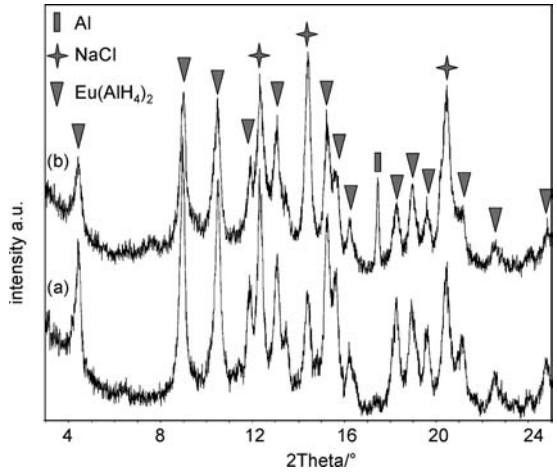

Figure 4. Powder XRD patterns obtained after ball-milling of (a) $NaAlH_4$ with $EuCl_2$ [$Eu(AlH_4)_2$-II] and (b) $NaAlH_4$ with $EuCl_3$ [$Eu(AlH_4)_2$-III] (Mo Kα_1 radiation).

DSC experiments (Figure 3) show for both samples, $Eu(AlH_4)_2$-II and $Eu(AlH_4)_2$-III, an exothermic reaction, starting at about 100 °C for $Eu(AlH_4)_2$-II. This is followed by an endothermic reaction, starting at about 180 °C for the particular measurement conditions. Both reaction steps are accompanied by hydrogen release. The decomposition enthalpies calculated from the DSC data are −4.4 kJ mol^{-1} of H_2 for the first reaction step and 57 kJ mol^{-1} of H_2 for the second step. For $Eu(AlH_4)_2$-III, an additional endothermic reaction with an onset at about 80 °C is observed, correlated to the decomposition of AlH_3.[13]

Synthesis of $Sr(AlH_4)_2$. The chemical similarity of europium and strontium encouraged us to prepare also strontium alanate starting from $NaAlH_4$ and $SrCl_2$. The successful preparation of $Sr(AlH_4)_2$ from $SrCl_2$ and $NaAlH_4$ by ball-milling is shown in Figure 5.

The thermal behavior for $Sr(AlH_4)_2$ is completely different, with a main exothermic reaction at about 130 °C and two endothermic reactions starting above 240 °C (Figure 6).

Thermolysis Data. For thermal desorption experiments, the samples were heated, and the hydrogen released was collected in a buret. This allows calculation of the amount of released hydrogen during different thermolysis steps. As was already discussed for the DSC experiment, thermolysis proceeds in two steps, with the first step releasing 0.6 wt % H_2 for $Eu(AlH_4)_2$-II and 0.8 wt % for $Eu(AlH_4)_2$-III. During the second step, about 1.1 wt % H_2 is released for $Eu(AlH_4)_2$-II and

dx.doi.org/10.1021/ic202492v | Inorg. Chem. 2012, 51, 4143–4150

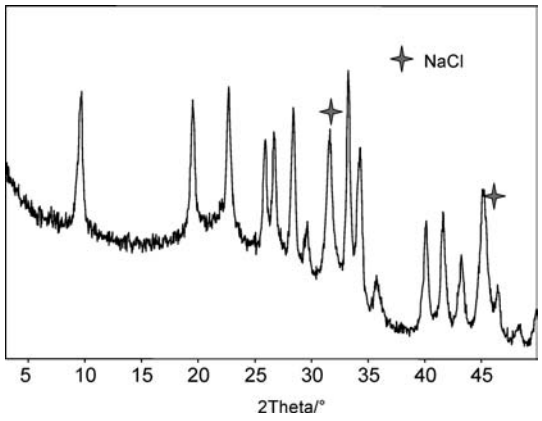

Figure 5. Powder XRD pattern of $Sr(AlH_4)_2$ after the preparation from $SrCl_2$ and $NaAlH_4$ (Cu Kα_1 radiation).

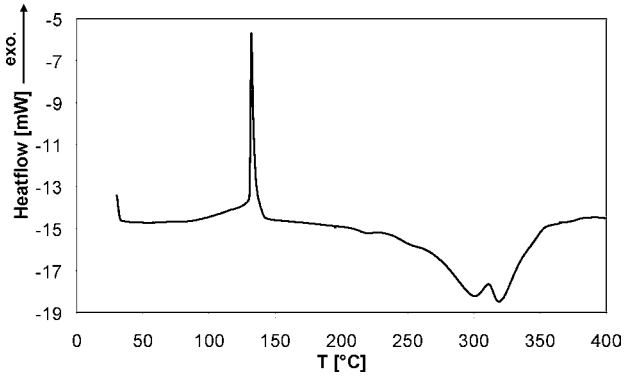

Figure 6. DSC curve of $Sr(AlH_4)_2$.

1.0 wt % for $Eu(AlH_4)_2$-III (Figure 7). During thermolysis of $Sr(AlH_4)_2$, the first 0.8 wt % hydrogen is released up to about 120 °C, and in a second step, 1.3 wt % hydrogen is released up to 300 °C. In addition to the thermolysis curves measured during the first dehydrogenation, a second thermolysis curve was recorded after rehydrogenation of all three samples. Rehydrogenation was performed at 30 MPa for 3 h. All values refer to the entire weight of the sample including Al and NaCl. The lower amount of released hydrogen of the dehydrogenated samples is discussed later in this paper.

In order to understand the hydrogen release in detail, powder XRD experiments were carried out. For this purpose, $Eu(AlH_4)_2$-II was filled into a capillary under a protective atmosphere. Then the sample was heated to distinct temperatures. After reaching the respective temperatures, the sample was cooled to room temperature and a data set was collected (Figure 8). The figure includes also the simulated powder XRD patterns of $Eu(AlH_4)_2$ and $EuAlH_5$ based on the crystal structure solution presented later in this paper.

The sample heated to 100 °C mainly consists of $Eu(AlH_4)_2$, but weak reflections at d = 4.3 and 6.3 Å have appeared that belong to a new phase, $EuAlH_5$. The amount of $EuAlH_5$ increases continuously, while $Eu(AlH_4)_2$ disappears. Keeping the sample isothermal at 140 °C for several hours shows that some time is needed until the decomposition of $Eu(AlH_4)_2$ to $EuAlH_5$ is completed (Figure 8), indicating very slow kinetics. Continuous heating to 600 °C reveals that $Eu(AlH_4)_2$ is stable up to 200 °C before the decomposition to $EuAlH_5$ is completed. A further increase of the temperatures leads to the decomposition of $EuAlH_5$, and at 300 °C, $EuAl_4$ is formed. Figure 9 compares the powder XRD patterns of $Eu(AlH_4)_2$ and

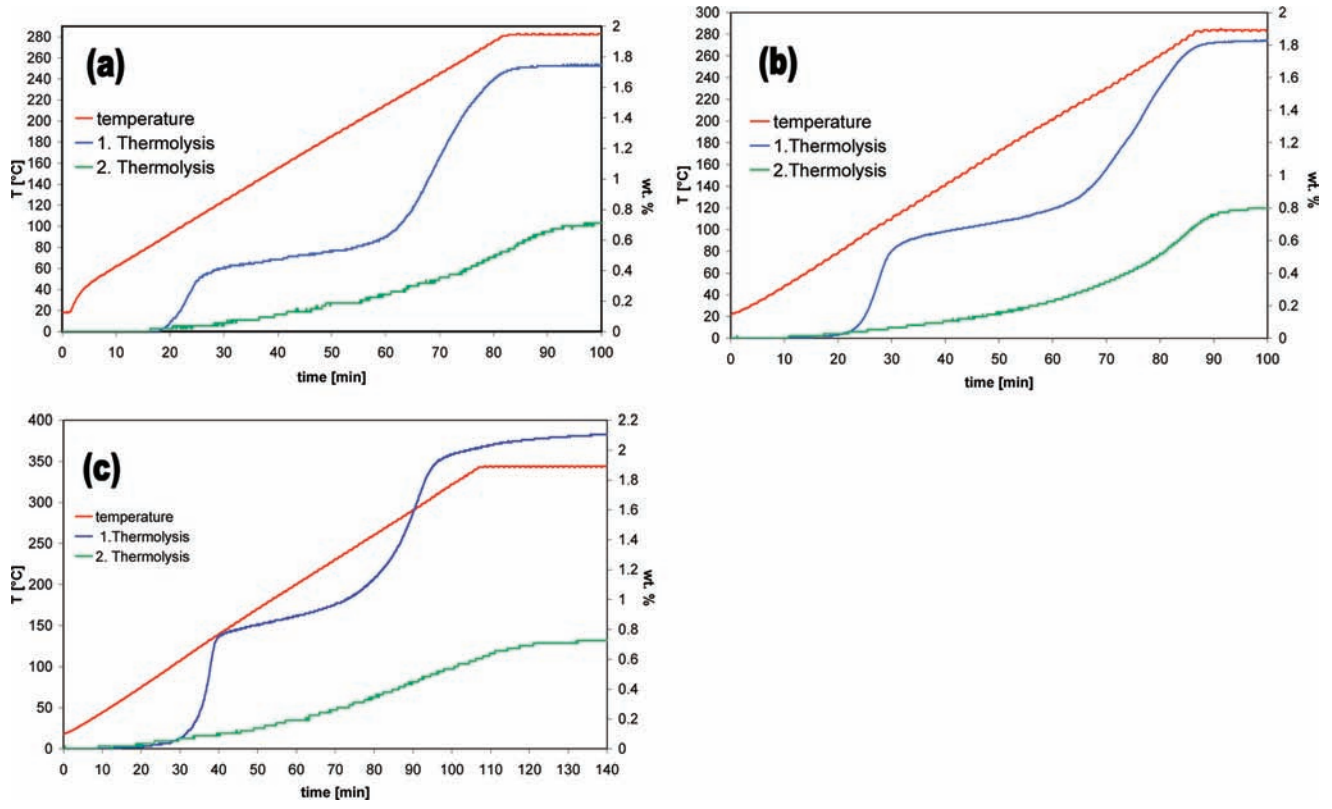

Figure 7. Thermolysis curves obtained during heating of (a) $Eu(AlH_4)_2$-II, (b) $Eu(AlH_4)_2$-III, and (c) $Sr(AlH_4)_2$. All graphs show also the amount of hydrogen released after rehydrogenation.

dx.doi.org/10.1021/ic202492v | *Inorg. Chem.* 2012, 51, 4143–4150

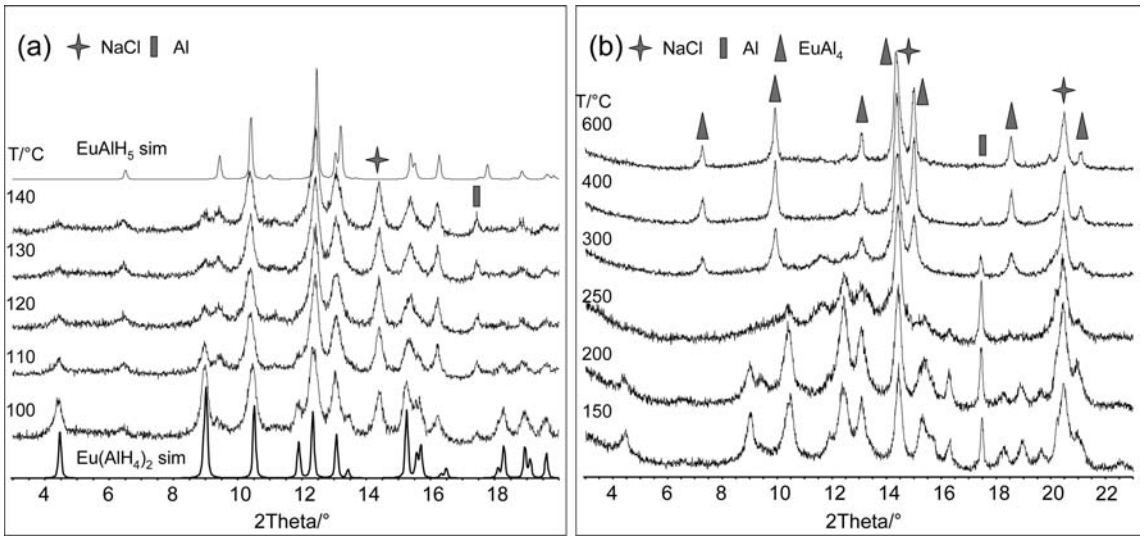

Figure 8. (a) Simulated (see section Crystal Structure Determination) powder XRD patterns of $Eu(AlH_4)_2$ (lower) and $EuAlH_5$ (upper) and selected powder XRD patterns collected after dehydrogenation at different temperatures. (b) Selected powder XRD patterns collected after dehydrogenation between 150 and 600 °C.

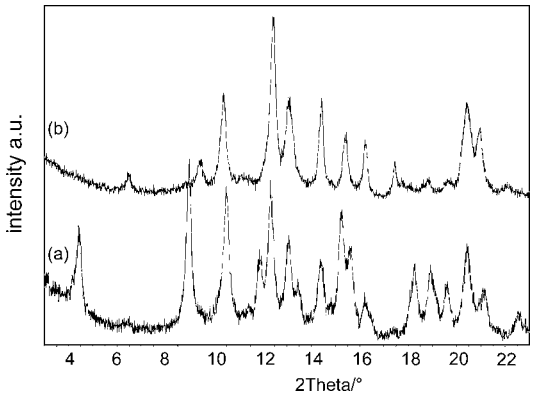

Figure 9. $Eu(AlH_4)_2$-II measured at higher resolution and better counting statistics at (a) room temperature and (b) after heating to 140 °C (the sample is then partly decomposed to $EuAlH_5$, Mo Kα_1 radiation).

$EuAlH_5$ measured at higher resolution and better counting statistics.

The powder XRD patterns measured during the stepwise dehydrogenation of $Sr(AlH_4)_2$ show qualitatively the phase changes with increasing temperature from $Sr(AlH_4)_2$ to $SrAlH_5$ (Figure 10).

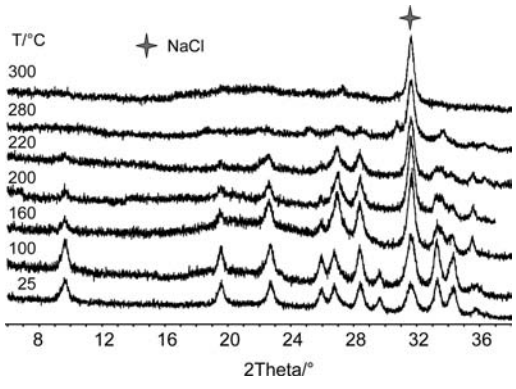

Figure 10. Powder XRD data collected under ambient conditions after heating of $Sr(AlH_4)_2$ to defined temperatures.

The pattern obtained after decomposition contains only reflections belonging to NaCl formed during synthesis and Al. No further decomposition products belonging to a strontium-containing phase can be verified. However, the high content of the amorphous material, indicated by the high background intensity in the range between about 15° and 30°, suggests that the strontium-containing phase might be amorphous.

Crystal Structure Determination. Indexing of the powder XRD pattern of $Eu(AlH_4)_2$ was performed after peak fitting using the program *FullProf*[14] with the program *CRYSFIRE*.[15] Only the McMaile algorithm using positions and intensities of the extracted reflections was able to find a unit cell for which the structure could be solved subsequently. Visual inspection of the match between the calculated cell and measured data was performed with the package *Checkcell*,[16] whereas the space group symmetry *Pnmm* was found manually on the basis of extinct reflections.[17] The positions of the heavy atoms were determined by simulated annealing methods, as implemented in the program *FullProf* without any constraints. The positions were subsequently refined by the Rietveld program implemented in the same program package (Figure 11). The powder XRD data of $EuAlH_5$ could not be indexed by any program, and a preliminary unit cell was derived from theoretical calculations based on the predicted crystal structure of $SrAlH_5$.[9] The structure solution was performed as described above in the suggested space group $P2_12_12_1$. Afterward, higher symmetry was detected using the *PLATON* program package[18] and the final space group *Pnma* was verified by Rietveld refinements. Rietveld refinements were performed for all structures, $Eu(AlH_4)_2$/$Sr(AlH_4)_2$ and $EuAlH_5$ (Figure 12), using pseudo-Voigt functions, manually chosen background points with refineable heights for the correction of the background, and isothermal displacement parameters for the Eu/Sr and Al atoms. From XRD data only, the positions of Eu/Sr and Al could be determined, while localization of the H positions from powder XRD data, in principle, is not possible. Localization of H atoms requires neutron diffraction data. For this, hydrogen has to be exchanged by deuterium. However, europium-containing phases are difficult to analyze because of their high neutron absorption cross section. After determination of the

dx.doi.org/10.1021/ic202492v | Inorg. Chem. 2012, 51, 4143–4150

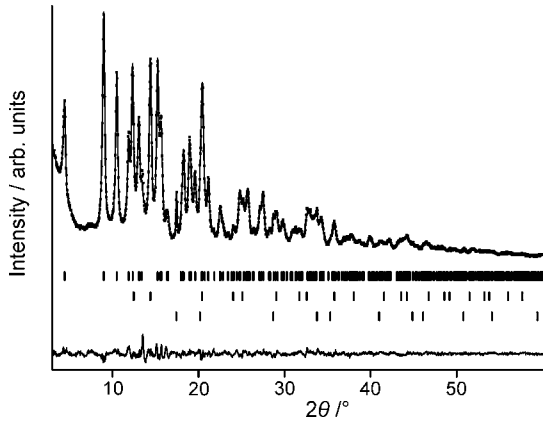

Figure 11. XRD pattern (λ = Mo Kα_1) of $Eu(AlH_4)_2$-II (black points), calculated pattern (black line), and difference between the observed and calculated patterns (lower black line) according to the final Rietveld refinement and theoretical Bragg positions (black tick marks) of $Eu(AlH_4)_2$, NaCl, and Al (from top to bottom).

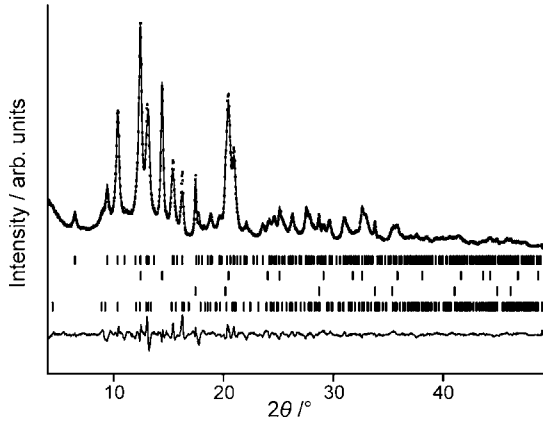

Figure 12. XRD pattern (λ = Mo Kα_1) after the sample was kept for 1 h at 140 °C (black points), calculated pattern (black line), and difference between the observed and calculated pattern (lower black line) according to the final Rietveld refinement and theoretical Bragg positions (black tick marks) of $EuAlH_5$, NaCl, Al, and $Eu(AlH_4)_2$ (from top to bottom).

crystallographic positions of the heavy atoms, the structure was refined from powder XRD data. The Rietveld plot of the refined crystal structure of $Eu(AlH_4)_2$, considering only the heavy atoms, is shown in Figure 11, and the crystallographic data are given in Table 1. While the positions of the heavy atoms can be determined, the orientation of the coordination polyhedron around the central Al atom cannot be confirmed without neutron diffraction experiments for localization of the D positions. As shown below, solid-state NMR spectroscopy helped to obtain more information about the crystal structure details. The refinement plot for the crystal structure of $Sr(AlH_4)_2$ is shown in the Supporting Information (Figure S2), and the crystallographic data are given in Table 1. Because of the poor crystallinity of the $SrAlH_5$ phase, no crystal structure refinements could be performed, but from the similarity of the diffraction pattern to $EuAlH_5$, the crystal structures are most probably isostructural. A comparison of the powder XRD patterns for $Eu(AlH_4)_2$/$Sr(AlH_4)_2$ and $EuAlH_5$/$SrAlH_5$ is given in the Supporting Information (Figure S3).

Solid-State ^{27}Al NMR Spectroscopy. While europium samples cannot be analyzed by NMR spectroscopy, strontium

Table 1. Crystallographic Data for $Eu(AlH_4)_2$, $EuAlH_5$, and $Sr(AlH_4)_2$: Space Group, Unit-Cell Parameters, Residual Values of the Rietveld Refinement, Positional Parameters (x, y, z), and Refined Isotropic Temperature Factors (B_{iso})

	$Eu(AlH_4)_2$	$EuAlH_5$	$Sr(AlH_4)_2$
space group	*Pnmm* (No. 59)	*Pnma* (No. 62)	*Pnmm* (No. 59)
a/Å	9.1003(13)	12.481(3)	9.1165(18)
b/Å	5.1912(8)	5.0103(12)	5.2164(11)
c/Å	4.2741(5)	4.5887(11)	4.3346(8)
V/Å^3	201.81(4)	286.95(12)	201.81(4)
R_{wp}/%	8.4	9.5	13.4
R_B/%	3.2	2.8	5.0

	x	y	z	B_{iso}/Å^2
		$Eu(AlH_4)_2$		
Eu	0.1966(3)	$^1/_4$	$^3/_4$	1.6(1)
Al1	0.9625(12)	$^1/_4$	$^1/_4$	2.6(2)[a]
Al2	0.3821(15)	$^3/_4$	$^1/_4$	2.6(2)[a]
		$EuAlH_5$		
Eu	0.6517(3)	$^1/_4$	0.0216(12)	1.5(2)
Al	0.4105(14)	$^1/_4$	0.586(4)	2.5(3)
		$Sr(AlH_4)_2$		
Sr	0.1958(3)	$^1/_4$	$^3/_4$	1.5(1)
Al1	0.9665(11)	$^1/_4$	$^1/_4$	2.4(2)[a]
Al2	0.37309(11)	$^3/_4$	$^1/_4$	2.4(2)[a]

[a]Restrained to the same value.

alanate can be analyzed. Most probably, the crystal structure is built of isolated AlH_4 tetrahedra. To confirm the coordination of aluminum and the connectivity between the individual polyhedra, solid-state ^{27}Al NMR spectra were recorded. The spectrum of $Sr(AlH_4)_2$ collected at room temperature shows two signals with chemical shifts of 103 and about 9 ppm (Figure 13). The first signal is assigned to isolated $[AlH_4]^-$

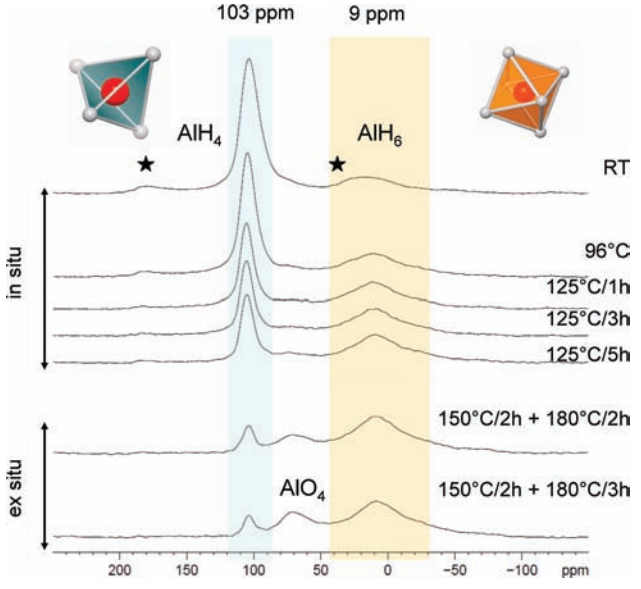

Figure 13. ^{27}Al NMR spectra. The asterisks indicate the spinning sidebands of the line at 109 ppm expected to be at ~180 and 26 ppm.

tetrahedra, while the second one is related to $[AlH_6]^{3-}$ octahedra. The octahedra seem to be corner-sharing. In addition to the room temperature spectrum, several spectra were collected in situ at elevated temperatures; two spectra

dx.doi.org/10.1021/ic202492v | Inorg. Chem. 2012, 51, 4143–4150

were collected after ex situ heating to 180 °C and subsequent cooling. Clearly visible is the increase of the signal intensity belonging to Al in octahedral coordination at the expense of the Al signal arising from a tetrahedral arrangement.

The experimental results obtained so far reveal that the crystal structures of europium and strontium alanate most probably consist of isolated $[AlH_4]^-$ tetrahedra, while the structures of the intermediate decomposition products $EuAlH_5$/$SrAlH_5$ are composed of corner-sharing $[AlH_6]^{3-}$ octahedra. The experimental structures are very similar to the crystal structure predicted for $SrAlH_5$[9] except for the fact that the structure of $EuAlH_5$ can be described in higher symmetry. In the predicted structure, $[AlH_6]^{3-}$ units are corner-sharing and form zigzag chains along the *c* axis. In the experimental structure, neighboring Al atoms are located at a distance of about 3.4 Å along the *b* axis. The Al atoms are positioned in such way that a zigzag arrangement of $[AlH_6]^{3-}$ is possible. A simulation of the powder patterns considering only the heavy atoms shows significant differences between the two structures (Figures 14 and 15).

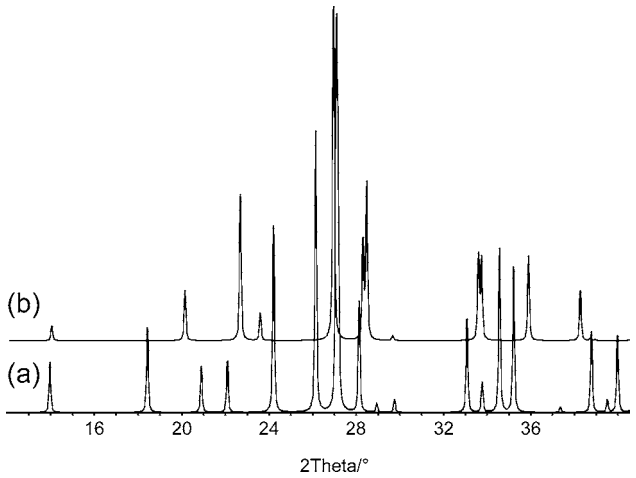

Figure 14. Simulated powder patterns for $SrAlH_5$ including only the heavy atoms: (a) $P2_12_12_1$ (Klaveness et al.[9]); (b) *Pnma* structure based on the experimental data of this work.

The crystal structures of the $SrAl_2H_2$ hydride and of the deuterated sample were solved from Patterson maps.[4] The structure can be deduced from the $SrAl_2$ structure, which can be described as a hexagonal net of covalently bonded Al atoms with three bonds within the hexagonal net and one bond in the neighboring net below or above. This results in the formation of a three-dimensional polymer Zintl anion. During hydrogenation, the bonds within the hexagonal net are retained, while the fourth bond to an Al atom in the adjacent net is replaced by a bond to one H atom. Sr_2AlH_7 and deuteride crystallize in the trigonal space group $P\bar{3}m1$, and they contain two-dimensional polymer Zintl anions in which one hydrogen/deuterium is covalently bonded to each Al atom. During further hydrogenation, a ternary alanate is formed. The structure consists of isolated $[AlH_6]^{3-}$ units and infinite one-dimensional twisted chains of edge-sharing $[HSr_4]$ tetrahedra.[5] The H atom not only forms bonds with Al atoms but also with Sr, which results in the formation of $[HSr_4]$ tetrahedra.

Rehydrogenation Experiments. Rehydrogenation experiments were performed in a pressure mill at different hydrogen pressures and for different hydrogenation times. One sample was hydrogenated under static conditions at 100 MPa hydrogen pressure. Depending on the hydrogenation conditions, the sample composition changes significantly (Figure 16). Rehydrogenation under elevated pressures in a ball mill leads to the disappearance of the $EuAl_4$ reflections. Instead of the intermetallic compound, reflections of metallic aluminum and a broad amorphous hump between 2θ = 8 and 16° appeared in the diffraction patterns (for Mo radiation). The sample rehydrogenated for 3 h at 30 MPa was thermolyzed for a second time (Figure 7b), and 0.8 wt % H_2 was released. This is proof that partial rehydrogenation can be achieved. However, the phases formed cannot be assigned unambiguously. Rehydrogenation tests in the ball mill performed for 15 h and more do not result in rehydrogenation products that are easier to identify, but abrasion of the milling vessel appears. Hydrogenation under static conditions failed even after the application of 100 MPa hydrogen pressure.

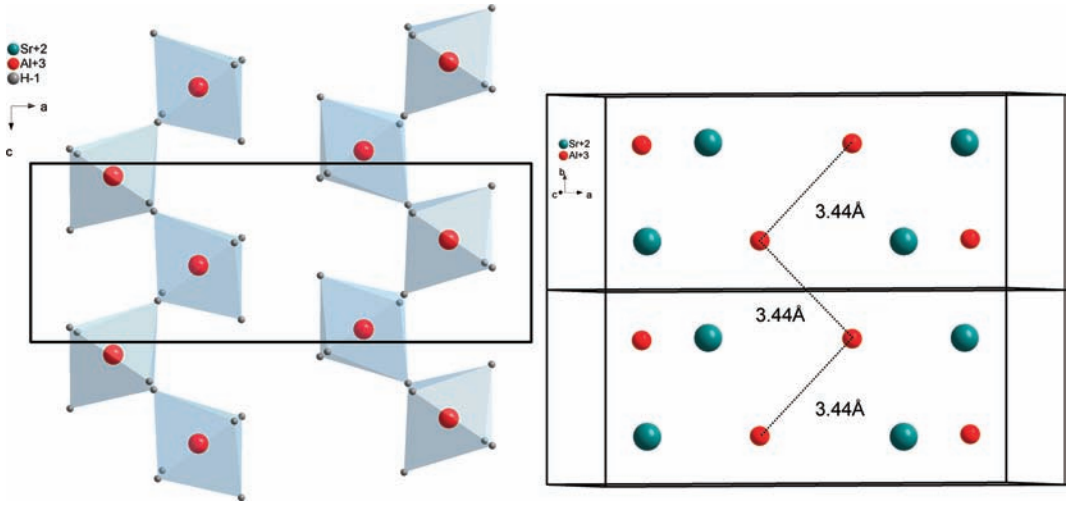

Figure 15. Crystal structure plot of $SrAlH_5$ predicted by Klaveness et al.[9] (left) and positions of the heavy atoms within the unit cell for $EuAlH_5$/$SrAlH_5$ (right). The bond distance of 3.44 Å plotted between the neighboring Al atoms corresponds to the distance between neighboring Al atoms in a zigzag chain formed by corner-sharing octahedra.

dx.doi.org/10.1021/ic202492v | *Inorg. Chem.* 2012, 51, 4143–4150

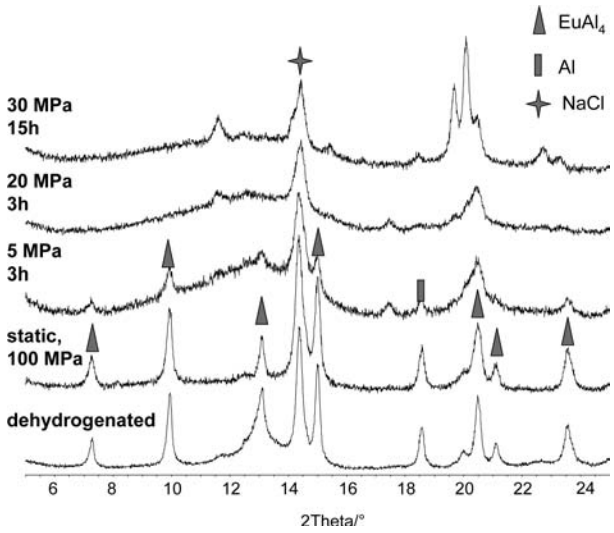

Figure 16. Powder XRD patterns collected after treatment of the dehydrogenated $Eu(AlH_4)_2$ at elevated hydrogen pressures. The additional strong peaks in the pattern collected after 15 h of milling time belong to steel reflections.

CONCLUSION

Complex aluminum hydrides with the composition $Me(AlH_4)_2$ (Me = Eu, Sr) were prepared by a mechanochemical metathesis reaction from $NaAlH_4$ and Eu/Sr chlorides. The crystal structures were solved from powder XRD data in combination with solid-state ^{27}Al NMR spectroscopy. The orthorhombic structure of $Eu(AlH_4)_2$, built up of isolated $[AlH_4]^-$ tetrahedra, starts to decompose at about 100 °C, and an intermediate phase of the composition $EuAlH_5$ is formed. The final decomposition product is an intermetallic compound with the composition $EuAl_4$. The structures of the Sr−Al compounds are isotypic to the europium compounds. However, thermolysis leads to the formation of aluminum as a crystalline product; a crystalline strontium-containing phase cannot be detected. Rehydrogenation experiments of the intermetallic $EuAl_4$ compound lead to a significant change of the powder XRD patterns, indicating a partial rehydrogenation of the material. The formation of EuH_x phases seems to be most likely. The first step of dehydrogenation from the alanate to the intermediate product is an exothermic reaction that makes rehydrogenation under reasonable conditions impossible. Rehydrogenation experiments indicate that the second decomposition step is reversible, but the amount of hydrogen released during this step is by far too low to consider these new aluminum hydrides as potential solid-state hydrogen-storage materials. The existence at least of $SrAlH_5$ has already been predicted by theoretical calculations, and this work contributes the experimental evidence for the existence of strontium and europium aluminum hydrides. The family of strontium aluminum hydrides is complemented by two new members, $Sr(AlH_4)_2$ and $SrAlH_5$.

ASSOCIATED CONTENT

Supporting Information

Simulated and measured powder XRD patterns and a Rietveld refinement plot for $Sr(AlH_4)_2$. This material is available free of charge via the Internet at http://pubs.acs.org.

AUTHOR INFORMATION

Corresponding Author

*E-mail: weidenthaler@kofo.mpg.de.

Notes

The authors declare no competing financial interest.

ACKNOWLEDGMENTS

We thank Bodo Zibrowius for the NMR spectroscopy.

REFERENCES

(1) Bogdanović, B.; Schwickardi, M. *J. Alloys Compd.* **1997**, *1*, 253.
(2) Mamatha, M.; Weidenthaler, C.; Pommerin, A.; Felderhoff, M.; Schüth, F. *J. Alloys Compd.* **2006**, *416*, 303.
(3) Weidenthaler, C.; Pommerin, A.; Felderhoff, M.; Sun, W. S.; Wolverton, C.; Bogdanović, B.; Schüth, F. *J. Am. Chem. Soc.* **2009**, *131*, 16735.
(4) Gingl, F.; Vogt, T.; Akiba, A. *J. Alloys Compd.* **2000**, *306*, 127.
(5) Zhang, Q. A.; Nakamura, Y.; Oikawa, K. I.; Kamiyama, T.; Akiba, E. *Inorg. Chem.* **2002**, *41*, 6547.
(6) Zhang, Q. A.; Akiba, E. *J. Alloys Compd.* **2005**, *394*, 308.
(7) Zhang, Q. A.; Enoki, H.; Akiba, E. *J. Alloys Compd.* **2007**, *427*, 153.
(8) Zhang, Q. A.; Akiba, E. *J. Alloys Compd.* **2008**, *460*, 272.
(9) Klaveness, A.; Vajeeston, P.; Ravindran, P.; Fjellvag, H.; Kjekshus, A. *J. Alloys Compd.* **2007**, *433*, 225.
(10) Dymova, T. N.; Konoplev, V. N.; Sizareva, A. S.; Aleksandrov, D. P. *Russ. J. Coord. Chem.* **2000**, *26*, 531.
(11) Bellosta von Colbe, J. M.; Felderhoff, M.; Bogdanović, B.; Schüth, F.; Weidenthaler, C. *Chem. Commun.* **2005**, *37*, 4732.
(12) Wickleder, M. S.; Meyer, G. *Z. Anorg. Allg. Chem.* **1996**, *622*, 593.
(13) Graetz, J.; Reilly, J. J. *J. Phys. Chem. B* **2005**, *109*, 22181.
(14) Rodriguez-Carvajal, J. *Phys. B* **1993**, *192*, 55.
(15) Shirley, R. *The CRYSFIRE System for Automatic Powder Indexing: User's Manual*; The Lattice Press: Surrey, England, 2000.
(16) Laugier, J.; Bochu, B. *LMGP—Suite of Programs for Interpretation of X-ray Experiments*; ENSP/Laboratoire des Materiaux et du Genie Physique: Saint Martin d'Heres, France, 2004.
(17) Hahn Th, Ed. *International Tables for Crystallography*, first online edition; Springer: Dordrecht, The Netherlands, 2006; Vol. *A*.
(18) Spek, A. L. *J. Appl. Crystallogr.* **2003**, *36*, 7.